Shear structures and microstructures in micaschists: the Variscan Cévennes duplex (French Massif Central)

F. Arnaud[a,b,*], A.M. Boullier[c], J.P. Burg[d]

[a]*Centre de Recherches Pétrographiques et Géochimiques, BP20, F-54501 Vandoeuvre-lès-Nancy, France*
[b]*La Fare, F-48370, Saint-Germain-de-Calberte, France*
[c]*Laboratoire de Géophysique Interne et Tectonophysique, BP53X, F-38041 Grenoble cedex 9, France*
[d]*ETH Zentrum, Sonneggstr. 5, Zürich 8092, Switzerland*

Abstract

Structural, microstructural and quartz ⟨c⟩ axis orientations have been investigated in shear zones within the Cévennes micaschist series (southeastern French Massif Central). These shear zones define a hinterland-dipping duplex formed during crustal thickening. They are characterised by superposed cleavages, a well-defined stretching lineation, isoclinal folds, shear planes and abundant quartz lenses. These shear zones were formed under P–T metamorphic conditions of ca. 500 °C and 450 MPa. The dominant deformation mechanism was dissolution–crystallisation. Fluid circulation responsible for element transfer was limited in space and dissolved silicate minerals are now found in the quartz lenses. Study of the syntectonic quartz lenses suggests fluid overpressure that has favoured brittle behaviour of the rock and formation of quartz lenses at different stages of the shearing event. Quartz lenses have accentuated the initial anisotropy of the micaschists and have strongly enhanced folding, boudinage and the development of shear zones. These deformation criteria for shear zone recognition can be applied in understanding the structure and significance of monotonous micaschist series in orogenic belts.
© 2004 Elsevier Ltd. All rights reserved.

Keywords: Shear zones; Monotonous micaschist series; Quartz lenses; Recognition criteria; Deformation mechanisms; Variscan belt; Fluid pressure

1. Introduction

Thick series of metapelitic schists commonly constitute slaty forelands of orogenic belts. The homogeneity of micaschist series with few lithological horizons resulted in limited interest for structural studies.

The apparent excessive thickness of the Cévennes series in the southern French Massif Central (Variscan belt) (Fig. 1) was interpreted as the result of isoclinal recumbent folds (Demay, 1931, 1948; Brouder, 1968; Munsch, 1981). However, large-scale fold hinges are not found in the field or determined by mapping reconstruction. Numerous syntectonic quartz lenses are concentred in ca. 100-m-thick zones, which are continuous on a regional scale. Although there is some variation according to the geological setting, studies in Variscan and Himalayan schists belts have shown that zones of high concentration of quartz

lenses are characterised by a strain gradient and sense-of-shear indicators (Sauniac, 1980, 1981). Therefore, Sauniac interpreted these zones as shear zones and explained the lenses by quartz crystallisation in openings originated during progressive shearing. The characteristics of shear zones in schists series are focussed on particular structures such as extensional crenulation cleavage (Platt and Vissers, 1980; Dennis and Secor, 1987) or microstructures (Lister and Snoke, 1984; Hippertt, 1994). The theoretical approach of Bell and Cuff (1989) predicted that dissolution–crystallisation is the dominant deformation mechanisms in such lithologies at all metamorphic grades. Microstructures and ⟨c⟩ axis preferred orientations are consistent with this hypothesis at low grade and retrograde metamorphic conditions (Hippertt, 1994). However, structural or microstructural studies have been seldom performed on micaschist shear zones formed under higher P–T conditions. The escape of large volumes of fluids during prograde metamorphic reactions and the increasing anisotropy of the rocks during progressive deformation have certainly

* Corresponding author. Correspondence address: La Fare, F-48370, Saint-Germain-de-Calberte, France. Tel.: +33-04-66-45-99-40.
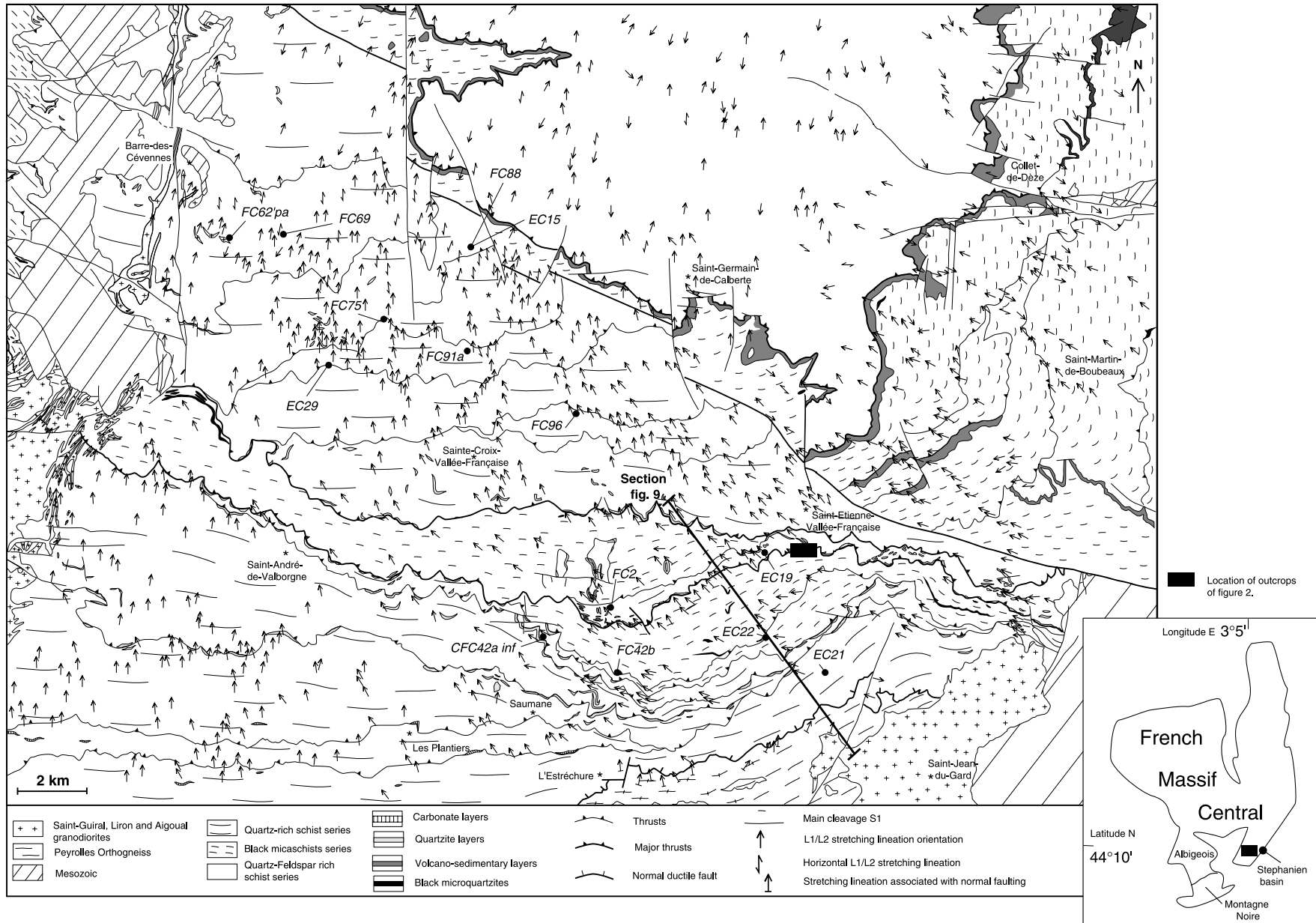*E-mail address:* arnaud@dstu.univ-montp2.fr (F. Arnaud).

Fig. 1. Geological and structural map of the Cévennes region and its location within the French Massif Central. Numbers refer to studied samples. The lithological levels are drawn after Brouder (modified, unpublished map).

controlled the deformation mechanism, the rheological behaviour and the development of structures and microstructures in these shear zones (Simpson, 1998).

This paper examines schist shear zones which have formed at ca. 500 °C and ± 450 MPa. Recognition criteria, structural and microstructural characteristics of such shear zones are described; the deformation mechanisms and the formation of quartz lenses in these zones during the shearing event are discussed. The recognition and the mapping of these shear zones allow us to reconstruct the geometry and the lithological section of the Cévennes area and to better understand the significance of this area in the Variscan belt (Arnaud, 1997).

2. Geological setting

Cévennes series are correlated with the schist series of Albigeois to the West (Fig. 1). Both are structurally dominated by a southward thrust system (Guérangé-Lozes, 1987; Guérangé-Lozes and Pellet, 1990; Arnaud and Burg, 1993) between 340 and 330 Ma (Costa, 1990).

The Cévennes and Albigeois series are regarded as the Cambro-Ordovician, southern parautochtonous domain of the Variscan belt upon which high-grade nappes were emplaced (Burg and Matte, 1978; Ledru et al., 1989; Costa, 1990; Matte, 1991; Quenardel et al., 1991; Costa et al., 1993). The allochthonous nappes include high-grade gneisses and mafic–ultramafic rocks with high pressure relicts (Gardien et al., 1988) and overlies the Cévennes and Albigeois units by over 200 km at least, as indicated by numerous klippes, with an average displacement to the south (Burg and Matte, 1978). To the south, the Cévennes and Albigeois series were thrust over the so-called Le Vigan and Monts-de-Lacaune series, respectively, which are themselves involved in the general south-verging nappe system (Demay, 1948; Alabouvette et al., 1988). The Monts-de-Lacaune series is believed to have been thrust onto the south-verging fold-nappes of the Montagne Noire (Arthaud, 1970) which are about 310 Ma old (Engel et al., 1981). Therefore, the parautochtone domain is thrust on more external domains that are themselves structured in the thrust system. The associated deformation and metamorphism are lower and younger (from 360 to 310 Ma) from north to south (Costa, 1990).

In the parautochtonous domain, prograde Barrovian metamorphism is associated with thrusting and decreases from middle-grade in the Cévennes (Arnaud, 1997) to very low-grade in the Montagne Noire (Engel et al., 1981).

Nappe emplacement was followed, in the Cévennes, by granodiorite intrusions between 330 and 300 Ma (Vialette and Sabourdy, 1977a,b; Mialhe, 1980; Najoui, 1996; Najoui et al., 2000). These granitoids are responsible for metamorphic aureoles superimposed on the regional metamorphism and have been attributed to syn- to post-orogenic extensions of the Variscan belt between 330 and 305 Ma

(Burg et al., 1994; Faure, 1995). The region was later affected by normal and wrench faulting mostly associated with Stephanian sedimentation, during post-thickening extension (Burg et al., 1994; Faure, 1995; Djarar et al., 1996).

3. Structural description of the micaschists

The Cévennes micaschists series include a lower quartz-rich schist series separated from an upper black micaschists series by a 10–15 m quartzite layer.

The main structure in the Cévennes micaschist series is a low angle regional S1 slaty cleavage sub-parallel to bedding S0. Previous authors have described large recumbent, west-verging (Arthaud et al., 1969; Munsch, 1981) or south-verging fold nappes (Demay, 1948; Brouder, 1968, 1971; Pellet, 1972; Magontier, 1988) or shearing (Mattauer and Etchecopar, 1977) to explain lithological repetitions and the > 5000 m thickness of the series. More recent mapping depicted a regional schistosity deformed by, and associated with, ca. 100-m-thick shear zones that produced stacking of the lithologies in a S–SE-verging duplex system (Arnaud and Burg, 1993). The regional S1 and the shear zone foliation S2 are characterised by similar metamorphic parageneses: quartz, plagioclase (albite, oligoclase), muscovite, chlorite, biotite and sometimes garnet and chloritoid. Metamorphic conditions are similar over large distances. Geothermobarometric studies yield metamorphic temperatures of 500 ± 12 °C and pressures of 520 ± 80 MPa (Arnaud, 1997). The pressure conditions are supported and specified at 440 ± 30 MPa by primary fluid inclusions in apatite within syntectonic quartz lenses (Arnaud, 1997). ^{40}Ar/^{39}Ar geochronology on muscovite, biotite and amphibole indicates cooling ages between 340 and 330 Ma (Caron, 1994). The 343.1 ± 4.4 Ma age on amphibole (Caron, 1994) (closure temperature of 500–550 °C; Berger and York, 1981) dates the metamorphic peak (Arnaud, 1997).

4. Structural description of the micaschists

4.1. Regional characteristics

The regional slaty cleavage and the deformation localised in the shear zones are contemporaneous with middle-grade metamorphism as mentioned above (Arnaud, 1997). Mica clusters and elongated quartz grains define the L1 stretching lineation oriented EW (in the SE part of the area) to NS (in the E part of the area) (Fig. 1). Few centimetre to decimetre large isoclinal folds F1 display stretched limbs and slightly thickened hinges. Their axis orientation is NNW–SSE to NE–SW. Sedimentary structures such as cross- and graded-bedding indicate that the micaschist series are regionally normal with folds F1

verging ESE to SE. S0–S1 intersection lineations are parallel to local F1 fold hinges. Rare quartz lenses are parallel to S1.

4.2. Shear zones

Shear zones are continuous, with a few metre thick zones and are characterised by specific structures that are not found regionally.

4.2.1. F2 folds

F2 folds deform the regional S1 slaty cleavage together with its L1 lineation. F2 hinges are particularly well displayed by S1 parallel quartz lenses (Fig. 2a). Ranging in scale from centimetre to metre, the F2 folds are typically non-cylindrical, tight to isoclinal. The orientation of the curvilinear axes is asymmetric at 5–20°, with an anticlockwise relationship with respect to L1 (Fig. 3a). Since the micaschists have a normal polarity, the facing of F2 folds is towards the S–SW. A crenulation lineation is commonly parallel to the F2 axes. In places, conjugate folds are associated with conjugate crenulation lineations.

4.2.2. Crenulation cleavages

The crenulation cleavage S2 is common in the shear zones (Fig. 2b). It is parallel to the axial planes of F2 folds and is systematically dipping steeper to the N than S1 (Fig. 3b). S2 may be concentrated in F2 fold hinges but usually occurs over the whole thickness of the shear zone. Where S2 is restricted to folds hinges, the cleavage outside the fold is S1. S1 appears in microlithons between S2 planes and the obliquity between both planes can be mistaken for S–C-type structures (Fig. 4). In the limbs of isoclinal F2 folds the cleavage is an S0–S1–S2 composite plane. In some places, more than two cleavages are developed. The obliquity of the successive crenulation cleavages is such that the youngest is the steepest, dipping to the N.

4.2.3. Stretching lineation and boudinage structures

Elongated quartz lenses (Fig. 2c) and quartz fibres define a marked stretching lineation L2 in the shear zones. The direction of L2 is on average close to L1 (Fig. 3c). Foliation boudinage corresponds to decimetric to metric pinch and swell structures.
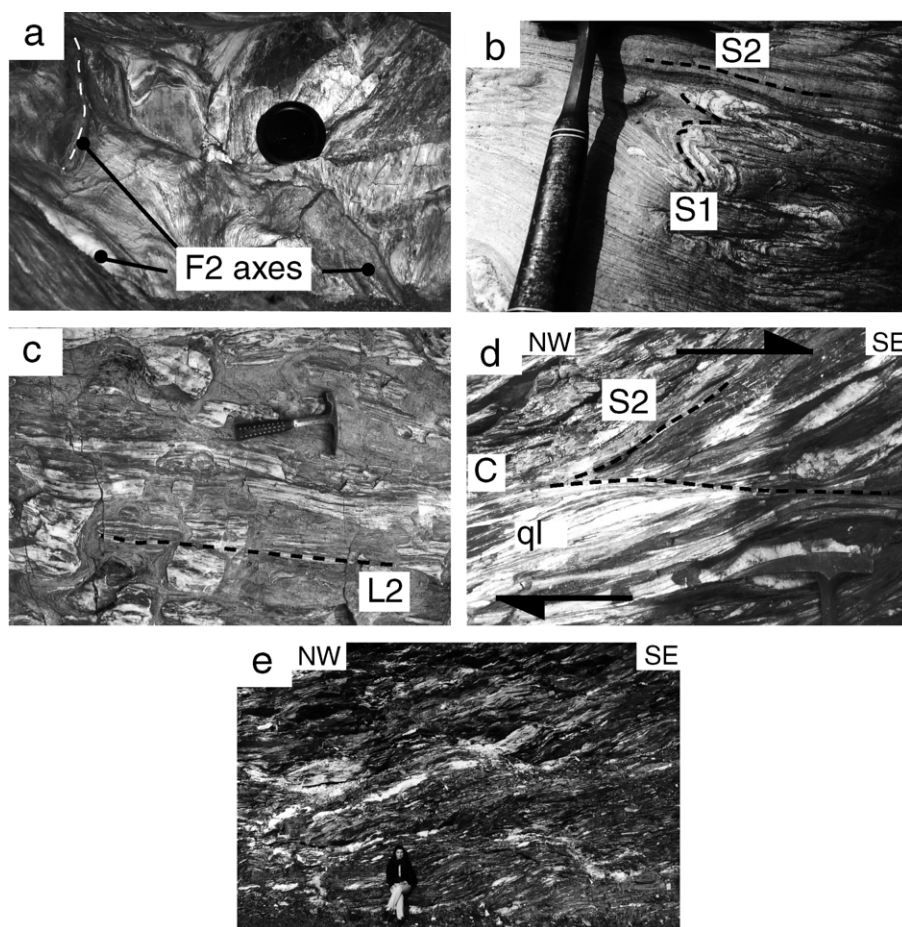

Fig. 2. Characteristic structures of the shear zones (Martinet, south of saint-Étienne vallée Française). (a) F2 fold axes of S1-parallel quartz lens. (b) Generalised S2 cleavage: S1 appears as microlithons between centimetric spaced S2 planes. (c) L2 stretching lineation marked by elongated quartz lenses. (d) Shear plane (C) affecting a S2 cleavage and quartz lenses (ql). (e) Concentration of syn-tectonic quartz lenses in schist shear zone. The schists are affected by numerous discontinuous shear planes that give a typical asymmetric 'button schists' outcrop.
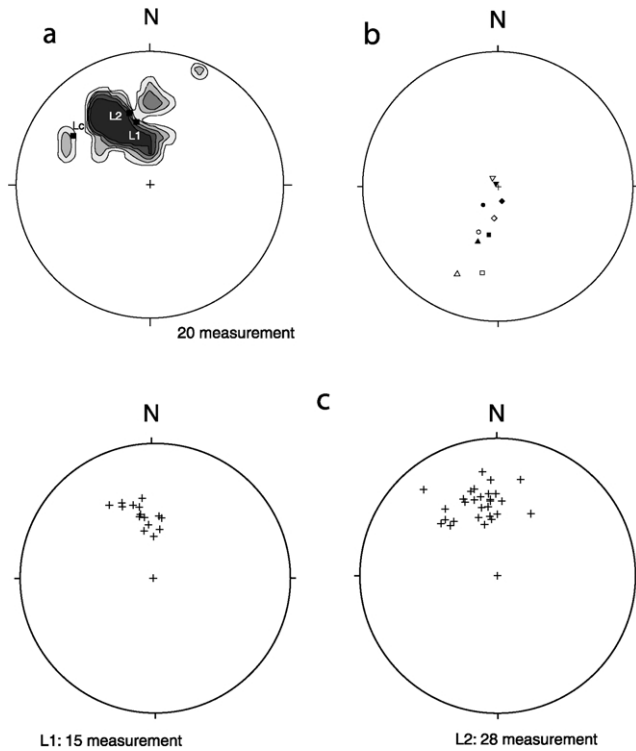
Fig. 3. (a) Schmidt density diagram of F2 axes in an outcrop (lower hemisphere, contours at 2, 6, 10, 14 and 18% per 1% area). L1 represents the main orientation of regional lineation marked by stretched minerals on S1 planes (16 meas.). L2 represents the main orientation of the stretching lineation marked by quartz fibres on quartz lenses (29 meas.). Lc represents the average crenulation lineation on S1 (10 meas.). (b) Schmidt diagram of S1 and S2 (lower hemisphere). Each symbol indicates an outcrop, the white one is the S1 and the black one is the S2. (c) Schmidt diagrams of lineations L1 and L2 on the Col du Pas outcrop (lower hemisphere).

4.2.4. The development of shear planes

Shear planes are abundant and contain muscovite, chlorite and eventually biotite The shear planes are discontinuous and their spacing is usually at the centimetre scale. In outcrops parallel to L1–L2 stretching lineations are characteristics, S1 and/or S2 foliations bend into the shear planes yet show an outcrop scale angular relationship of about 30° (Fig. 2d). Both the bending of foliations and the bulk angular relationship indicate a top-to-the-S to SE shear
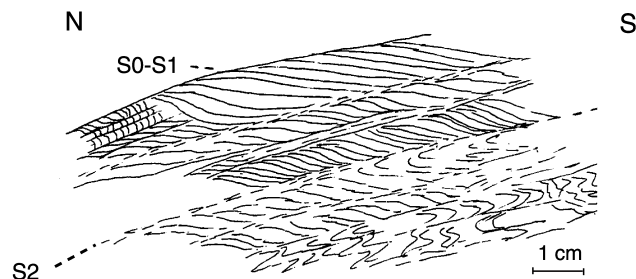

Fig. 4. Sketch of a large thin section in a F2 hinge showing relationships between S1 and S2. The apparent obliquity between S1 and S2 may lead to a confusing interpretation in term of S–C planes, which will indicate a wrong north verging shear sense.

sense depending on the stretching lineation direction. Quartz lenses are strongly stretched and thinned towards and into the shear planes. When shear planes at both extremities affect a quartz lens, the latter has an asymmetric shape consistent with a thrusting towards the S–SE (Fig. 2d).

4.2.5. Quartz lenses

A noticeable criterion to identify shear zones is the abundance of quartz lenses (Fig. 2e). They are millimetres to decimetres thick and centimetres to metres long. They represent up to 50% of the volume of the shear zone rocks, and show varying relationships with other shear structures. Most of the quartz lenses are parallel to S1 and are deformed with it. Some are folded (F2), some form rods defining the stretching lineation, and others are sheared as described above. Some are parallel to the local S2 and/or to shear planes. All these characteristics suggest that quartz lenses have been formed at different stages of the shearing event.

5. Microstructures in the shear zones

5.1. Micaschists

Foliation planes are defined by basal planes of muscovite, chlorite and biotite crystals and by flattening of quartz and plagioclase grains Two kinds of muscovite are observed: S1 grey muscovite platelets in microlithons and large and clear S2 muscovite flakes. S1 muscovites are abruptly truncated by the S2 muscovite grains (Fig. 5a). The angle between S1 and S2 varies between 45 and 90°. Some thin infra-millimetre quartz lenses parallel to S1 are folded and appear as microlithons between the S2 planes. They are truncated and apparently shifted by the S2 cleavage (Fig. 5b). In the microlithons, quartz grains do not show elongation, lattice preferred orientation or grain-size reduction near the S2 planes, their extinction is homogeneous. S2 is characterised by a high concentration of insoluble minerals (tourmaline, zircon), iron oxides and mica flakes compared with the microlithons (Fig. 5a).

5.2. Quartz lenses

5.2.1. Mineralogical composition

Beside quartz, albite, muscovite, chlorite, biotite and calcite are frequent with apatite and oxides as accessory minerals Companion minerals of quartz reflect the composition of the surrounding micaschists (Table 1) This is well illustrated by the (EC21) quartz lens that contains quartz, plagioclase, muscovite, chlorite, amphibole, calcite, oxides and accessory minerals (tourmaline, zircon) as found within the surrounding micaschists. Microprobe analysis indicates that minerals have the same compositions in both the lenses and the surrounding micaschists, whatever the relationship with S1 or S2 foliations (Arnaud, 1997).
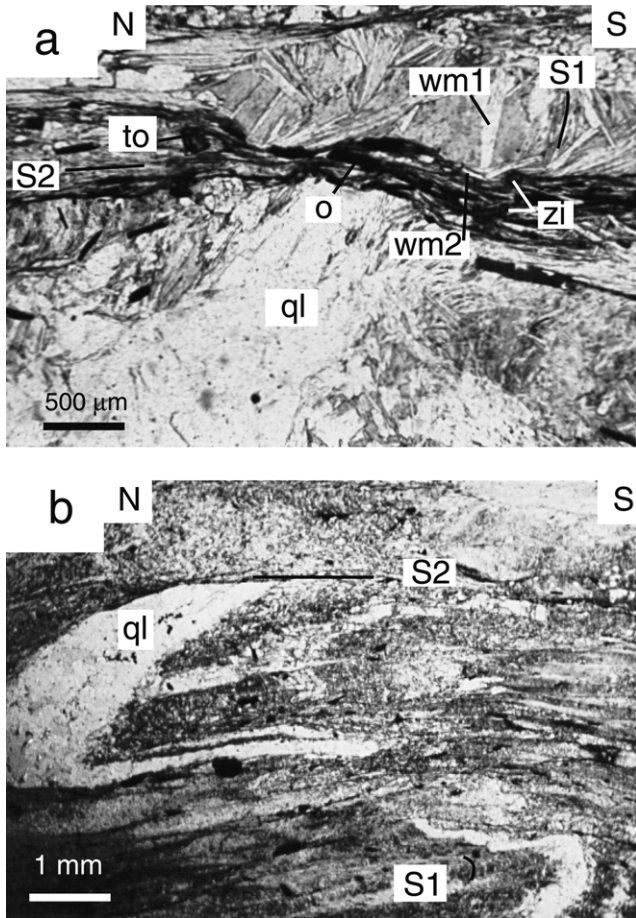
Fig. 5. Microphotographs showing the microstructures in micaschists. (a) Detail of relationships between S1 and S2 and between microlithons of quartz lenses parallel to S1 and S2. Contact between S1 and S2 is sharp. Syn-S1 white mica (wm1) is clearly cut by syn-S2 white mica (wm2). S2 is underlined by an abnormal concentration of insoluble minerals like oxides (o), zircon (zi) and tourmaline (to) (sample FC75). (b) Quartz lens (ql) parallel to S1 in a microlithon between S2 planes. The contact between the quartz lens and S2 is sharp and cut by S2 (sample FC69).

5.2.2. Wall-rock characteristics

As described above, the quartz lenses are mostly parallel to the S1 and/or S2 foliation planes. Recrystallised chlorite and muscovite, and locally biotite, coat the lens walls. These minerals appear as large and clean flakes. Some albite crystals have formed at the margins of the quartz lenses against the phyllite coating and display altered rims. Rosettes of calcite or chlorite are also present on the lens walls (Fig. 6a). The immediate wall-rock of some lenses is quartz-depleted and enriched in micas and dark insoluble minerals such as zircon, tourmaline and oxides.

5.2.3. Microstructures

Quartz lenses display predominantly a blocky milli-metric internal structure in which quartz grains are irregularly imbricated. Coarse-grained (0.5–0.7 mm) and

fine-grained (0.1–0.5 mm) microstructures are distin-guished (Figs. 7a and 8a and b). In fine-grained lenses, quartz grains are equant to slightly elongate. Grain boundaries are either straight (Fig. 8a) or slightly lobate (Fig. 8b) corresponding to grains with homogeneous or undulose extinction, respectively. Albite is idiomorph or ovoid with growth twins. Some albite crystals are elongated and form a discontinuous layer parallel to the wall-rock (Fig. 6b). Albite cores are cloudy due to the abundance of fluid inclusions, most of them being decrepitated. Chlorite is present in all quartz lenses and exhibits different shapes. Small flakes form fine bands parallel to the margins (Fig. 6c) in which chlorite may be associated with muscovite and/or biotite. These particu-lar zones are composed of finer-grained quartz and albite. Chlorite is also frequently observed in small zones made of numerous agglomerated crystals, or isolated with a caterpillar habit (ripidolite) characteristic of chlorite in hydrothermal veins. Little flakes of muscovite are frequently observed along grain bound-aries. Most of the quartz lenses include schist slivers that may exhibit two foliations, S1 within a microlithon and S2, parallel to the lens walls and to S2 within wall-rock (Fig. 6d). These schist slivers are essentially composed of phyllites with numerous accessory minerals and oxides.

5.2.4. Quartz preferred orientation

Fabrics were measured on thin sections cut parallel to the XZ planes of the strain ellipsoid. Cleavage and stretching lineation are oriented, respectively, parallel to the XY plane and X axis of the calculated finite strain ellipsoid. Quartz lenses with coarse-grained blocky microstructures have a crystal preferred orientation (CPO) with a maximum concentration of c-axis (7.5 and 9%) at 10–30° antic-lockwise to the stretching lineation (Fig. 7b). In quartz lenses with fine-grained blocky microstructures, the CPOs are less pronounced than in coarse-grained lenses (4.5–7% maxima). Two types of $\langle c \rangle$ axis fabrics have been recognised (Fig. 8c):

- The most frequent CPO shows two Z-centred small circles with a 20–40° opening angle (specimen FC62'pa, FC75, FC91a) and frequently connected through the bedding–cleavage intersection lineation (FC2, EC29, CFC42ainf). The maxima are generally localised at the outer rim of the diagram. In some samples, these maxima are asymmetric with either clockwise or anticlockwise angles with respect to Z (normal to S2).
- Some CPOs display an approximately asymmetric girdle passing through Y showing either a clockwise (EC22) or anticlockwise (EC21, CFC42b) rotation with respect to the cleavage plane.

Table 1
Comparison of the composition of the quartz lenses and wall rock at the thin section scale

Type of quartz lens		
Isoclinal fold	Shearing quartz lens	Lens
EC23: Qtz–Pl–Ms–Chl–Ap	FC39: Qtz–Ms–Zi	EC24: Qtz–Pl–Ms–Chl–Ap–To–Zi
EC25: Qtz–Pl–Ms–Bt–Chl–Cc–O	M: Qtz–Ms–Zi	M: Qtz–Pl–Ms–Chl–Ap–To–Zi
M: Qtz–Pl–Ms–Bt–Chl–To–O	CF13: Qtz–Pl–Ms–Bt–Chl–Ap	EC27: Qtz–Pl–Ms–Bt–Chl–Cc–Ap–FK
EC26: Qtz–Pl–Ms–Bt–Chl–Cc–Ap	M: Qtz–Pl–Ms–Bt–Chl–Ap–To–Zi	M: Qtz–Pl–Ms–Bt–Chl–Cc–Ap–To–FK
M: Qtz–Pl–Ms–Bt–Chl–Cc–Ap–To	EC19: Qtz–Pl–Ms–Chl–Ap–Zi	EC21: Qtz–Pl–Ms–Chl–Amp–Cc–Ap–O
EC20: Qtz–Pl–Ms–Chl–Cc	M: Qtz–Pl–Ms–Chl–Ap	M: Qtz–Pl–Ms–Bt–Chl–Amp–Cc–To–Zi–O
FC48: Qtz–Pl–Ms–Chl–Ap	FC2: Qtz–Ms–Chl	EC3: Qtz–Pl–Ms–Chl–Bt–Cc–Ap–To–Zi
M: Qtz–Pl–Ms–Chl–Ap–Zi–O	M: Qtz–Ms–Chl	EC7: Qtz–Pl–Ms–Bt–Chl–Ap–O
CFC42a: Qtz–Ms–Chl	EC22: Qtz–Ms–Chl	EC11: Qtz–Pl–Ms–Bt–Chl–Ap–O
M: Qtz–Ms–Chl–Ap–Zi–To–O	M: Qtz–Ms–Chl	M: Qtz–Pl–Ms–Bt–Chl–Ap–O
EC4: Qtz–Pl–Ms–Bt–Chl–Cc–Ap–O	CFC42b: Qtz–Ms–Chl	EC12: Qtz–Ms–Bt–Chl–Ap–O
M: Qtz–Pl–Ms–Bt–Chl	M: Qtz–Ms–Chl–To–Zi–O	M: Qtz–Ms–Bt–Chl–Ap–Zi–O
EC5: Qtz–Pl–Ms–Bt–Chl–Ap	EC14: Qtz–Pl–Ms–Bt–Chl–Ap	FC55: Qtz–Pl–Ms–Chl–O
M: Qtz–Pl–Ms–Bt–Chl–Ap–To–Zi	M: Qtz–Pl–Ms–Bt–Chl–Ap	M: Qtz–Pl–Ms–Bt–Chl–Ap–To–Zi–O
EC6: Qtz–Pl–Ms–Bt–Chl–Ap	EC15: Qtz–Pl–Ms–Bt–Chl–Ap	FC67': Qtz–Pl–Ms–Bt–Chl–Ap–Cc–O
M: Qtz–Pl–Ms–Bt–Chl–Ap–To–Zi	M: Qtz–Pl–Ms–Bt–Chl–Ap	M: Qtz–Pl–Ms–Bt–Chl–To–O
EC16: Qtz–Pl–Ms–Bt–Chl	FC71: Qtz–Pl–Ms–Chl–Grt–Ap	
M: Qtz–Pl–Ms–Bt–Chl–To–O	M: Qtz–Pl–Ms–Bt–Chl–Grt–Ap–O	
EC17: Qtz–Pl–Ms–Bt–Chl–Ap	FC80: Qtz–Pl–Ms–Chl	
M: Qtz–Pl–Ms–Bt–Chl–Ap–To–Zi	M: Qtz–Pl–Ms–Bt–Chl–Ap–To–Zi–O	
EC29: Qtz–Pl–Ms–Bt–Chl–Ap–To	FC88a: Qtz–Pl–Ms–Bt–Chl	
M: Qtz–Pl–Ms–Bt–Chl–To–Zi–O	M: Qtz–Pl–Ms–Bt–Chl–O	
FC58: Qtz–Pl–Ms–Bt–Chl	FC91a: Qtz–Pl–Ms–Bt–Chl	
M: Qtz–Pl–Ms–Bt–Chl–Ap–To–O	M: Qtz–Pl–Ms–Bt–Chl–O	
FC62': Qtz–Pl–Ms–Bt–Chl–Ap–O	FC91b: Qtz–Pl–Ms–Bt–Chl–O	
M: Qtz–Pl–Ms–Bt–Chl–Ap–To–Zi–O	M: Qtz–Pl–Ms–Bt–Chl–O	
FC73: Qtz–Pl–Ms–Chl–O	FC96: Qtz–Ms–Bt–Chl	
M: Qtz–Pl–Ms–Chl–To–Zi–O	M: Qtz–Pl–Ms–Bt–Chl–Ap–To–Zi–O	
FC75b: Qtz–Pl–Ms–Bt–Chl–Ap		
M: Qtz–Pl–Ms–Bt–Chl–Ap–To–Zi–O		
FC76: Qtz–Pl–Ms–Bt–Ap		
M: Qtz–Pl–Ms–Bt–Ap		
FC83: Qtz–Pl–Ms–Bt–Chl–Ap		
M: Qtz–Pl–Ms–Bt–Chl–To–O		
FC84: Qtz–Pl–Ms–Chl		
M: Qtz–Pl–Ms–Chl–Grt–O		
FC85: Qtz–Pl–Ms–Bt–Chl–Ap–O		
M: Qtz–Pl–Ms–Bt–Chl–O		
FC91c: Qtz–Pl–Ms–Bt–Chl–O		
M: Qtz–Pl–Ms–Bt–Chl–To–O		

Abbreviations: ECX: quartz lens in thin section ECX; M: schist in the same thin section ECX; Qtz: quartz; Pl: plagioclase; FK: K-feldspar; Ms: muscovite; Bt: biotite; Chl: chlorite; Amp: amphibole; Grt: garnet; Cc: calcite; Ap: apatite; Zi: zircon; To: tourmaline; O: opaques.

6. Interpretation and discussion

6.1. Large scale structures

The characteristics of younger cleavage systematically dipping steeper to the north than older ones, regional similarity between L1 and L2 stretching lineation trajectories and identical metamorphic conditions for both the S1 and S2 cleavages all suggest that these structures result from progressive deformation in a single regional shearing event (Arnaud, 1997) Shearing is initially responsible for the regional S1 slaty cleavage and its L1 stretching lineation Deformation is then concentrated in shear zones with S2 structures. Mapping shows that quartzite layers are repeated across these shear zones, which are interpreted as thrusts of a S- to SE-verging imbricate system (Fig. 9; Arnaud, 1997). This interpretation provides an explanation for the reportedly extreme thickness of the Cévennes micaschists.

6.2. Structures in shear-zones

This paragraph concerns the development of specific structures such as F2, S2, L2, crenulation lineation, boudinage and shear planes. F2 folds are similar to those described by Berthé and Brun (1980) and, following these
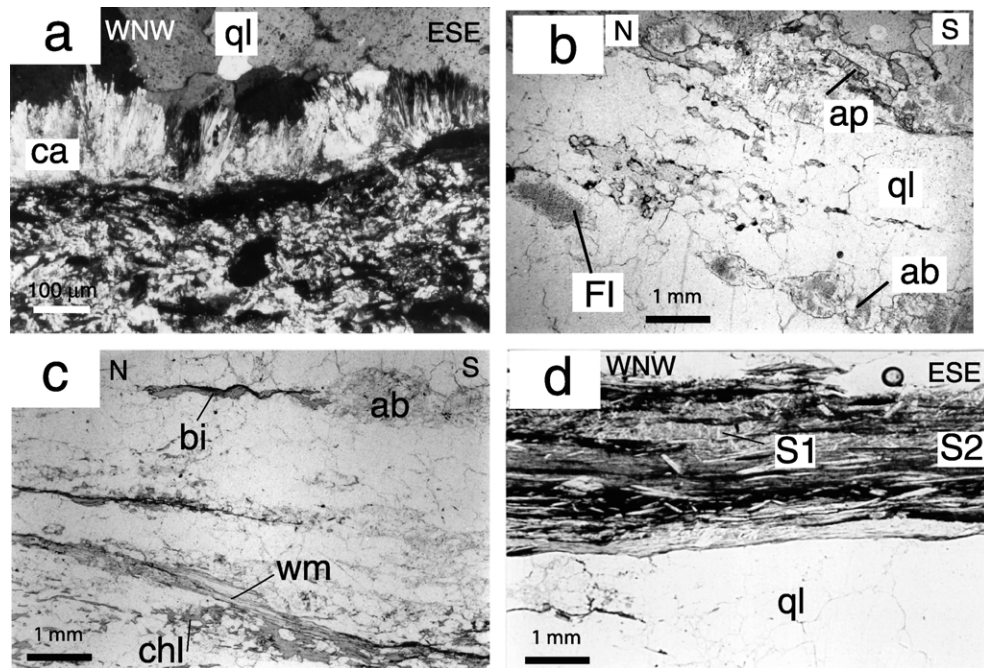
Fig. 6. Growth microstructures in quartz lenses. (a) Calcite with a fibrous and 'rosette' habit at the margin of a quartz lens (sample EC21). (b) Elongated crystals of albite (ab) aligned along bands parallel to the wall-rock. Note the grey colour of albite core due to decrepitated fluid inclusions (FI). Apatite (ap) is common in quartz lenses and is associated with albite (sample FC55). (c) Layers composed of albite (ab) and flakes of white mica (wm), chlorite (chl) and biotite (bt) and parallel to wall-rock. In these bands quartz grains have a reduced grain-size (sample FC88). (d) Sliver of micaschist parallel to the wall rocks, included in a quartz lens and in which two schistosities are observed, S1 microlithons between S2 planes, which are parallel to S2 in the wall-rock schists (EC22).

authors, are interpreted as initiated by shearing of heterogeneities in strongly anisotropic rocks. However, in the case of the Cévennes micaschists, the orientation of fold axes is relatively constant, at 10–30° anticlockwise from the L2 stretching lineation. This fact suggests that fold axes have probably formed initially oblique (ca. 30°) to the stretching lineation and then have been rotated towards the stretching direction in response to shear. Fold axes initiated oblique to the stretching lineation may reflect a wrenching component (Coward and Potts, 1983; Ridley, 1986) tentatively attributed to large dextral lateral ramps next to the Cévennes thrust system. F2 folding is synchronous to the axial planar S2 cleavage. Crenulation lineations, parallel to the F2 axes, represent microfolds of the S1 cleavage. Boudinage structures are similar to 'foliation boudinage', which have been described by Platt and Vissers (1980). Shear planes are interpreted as 'extensional crenulation cleavage'. The angular relationships between the shear zones, the shear planes and the S2 cleavage indicates that shear planes are also equivalent to the C' planes as defined by Berthé et al. (1979). These C' planes appear in response to a non-coaxial deformation of the anisotropic schists.

6.3. Quartz fabrics

The quartz $\langle c \rangle$ axis preferred orientations at low angle to the stretching lineation may be interpreted in different ways: (i) by prism $\langle c \rangle$ slip (Schmid et al., 1981; Mainprice et al., 1986), (ii) by competitive anisotropic growth during the dissolution–crystallisation process (Cox and Etheridge, 1983), (iii) by mechanical rotation of clastic grains during deformation so that the long axes, parallel to the $\langle c \rangle$ axis, became parallel to the stretching lineation (Stallard and Shelley, 1995), or (iv) by competitive anisotropic dissolution of quartz grains having their $\langle c \rangle$ axis parallel to the shortening direction (Hippertt, 1994). The P–T conditions under which the Cévennes quartz lenses have been formed and deformed are inconsistent with the known P–T field of prism $\langle c \rangle$ slip (Lister and Dornsiepen, 1982; Blumenfeld et al., 1986; Gapais and Barbarin, 1986; Mainprice et al., 1986). This type of CPO is observed in coarse-grained, i.e. apparently least deformed, quartz lenses. These CPOs are, therefore, interpreted to reflect the original, crystallisation orientation of quartz within the lenses where subsequent deformation by crystalline plasticity was not sufficient to induce a new quartz c-axis preferred orientation. This interpretation implies that the stretching lineation is the growth direction of quartz crystals within the lenses and has some consequences on the hypothesis for vein opening and sealing mechanisms.

The other quartz $\langle c \rangle$ axis preferred orientations correspond to fine-grained quartz lenses. The more deformed are the quartz lenses (isoclinal folds, stretched lenses), the finer is the grain-size. This observation suggests that grain-size reduction occurred by processes of crystal plasticity and dynamic recrystallisation (Poirier and Nicolas, 1975; Tullis et al., 2000). By analogy with computer simulations of quartz c-axis fabrics depending on the deformation paths
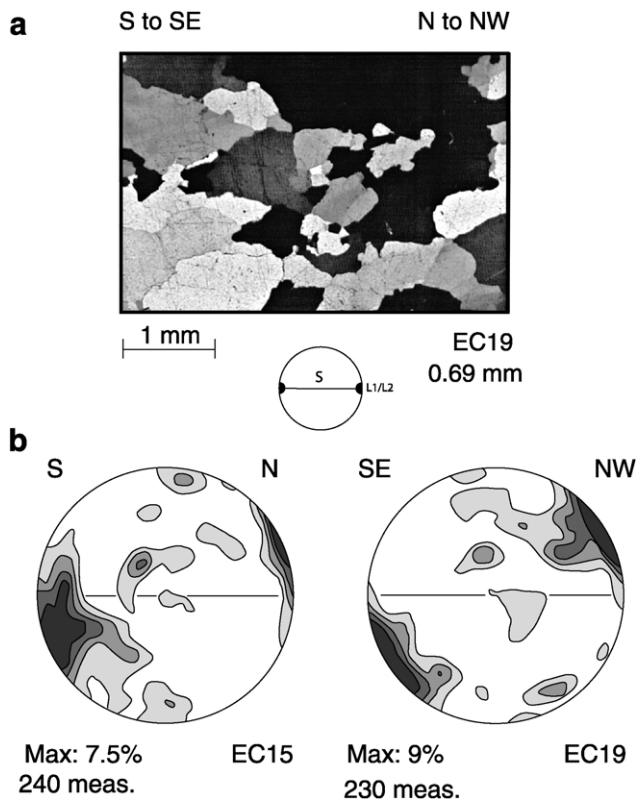
a

b

Fig. 7. Microstrutures (a) and typical c-axisPO of coarse quartz lenses (b). The $\langle c \rangle$ axis repartition and density contours (contours at 1, 2, 3, 4 and 8% per 1% area) have been reported on a Schmidt diagram (lower hemisphere) using the Fabric 7 program (Mainprice, 1992; unpublished). The EW line corresponds to the schistosity and the stretching lineation is horizontal in this plane.

and dislocation glide systems (Etchecopar, 1977; Lister and Hobbs, 1980; Etchecopar and Vasseur, 1987) and with studies of natural quartz fabrics (Marjoribanks, 1976; Schmid and Casey, 1986; Law et al., 1990; Passchier and Trouw, 1996), the asymmetric girdle determined in the Cévennes samples is interpreted in terms of non-coaxial deformation. According to the stretching lineation, this asymmetry in the Cévennes samples indicates a shear sense either top-to-the-S–SE or top-to-the-N–NW. Thus, folding after plastic deformation has probably modified the apparent shear sense and kinematic determination on the basis of quartz fabrics alone is not possible at this scale (Klaper, 1988). The frequent CPO characterised by a small circle around Z suggests a flattened strain ellipsoid (Tullis et al., 1973; Marjoribanks, 1976; B model of Lister and Hobbs, 1980; Law, 1986; Schmid and Casey, 1986; Passchier and Trouw, 1996). The maxima generally localised at the outer rim of the diagram indicate that basal $\langle a \rangle$ glide system was principally activated. In some diagrams, the occurrence of $\langle c \rangle$ axis in the Y position shows that prismatic $\langle a \rangle$ glide system was also activated. These systems are activated for deformation conditions which are compatible with the metamorphism in the Cévennes micaschists, i.e. between 400 and 500 °C.

6.4. Deformation mechanism in shear zones

In the literature, there are two hypotheses that explain the formation of quartz lenses in metamorphic zones: (i) quartz precipitation during metamorphic reaction following a change in P–T conditions (Goffé et al., 1987) and (ii) deformation by dissolution–crystallisation process (Durney, 1972; Gratier, 1984). In the Cevennes area, quartz lenses occur regardless of the composition of the surrounding rocks. However, quartz lenses are exclusively located within shear zones and structural relationships suggest that the quartz lenses were formed continuously during shearing. This supports the hypothesis of quartz lenses formed by the dissolution–crystallisation process.

The relationships between S1 and S2, the textures of microlithons between S2 planes and the concentration of insoluble minerals in S2 suggest that S2 formed by a dissolution process probably associated with metamorphic recrystallisation (Cox and Etheridge, 1989). The presence of synchronous S2 cleavage and quartz lenses in a small area is interpreted as coupled dissolution and crystallisation processes during shearing. The composition of quartz lenses, directly controlled by the composition of the immediate wall rock (Table 1) supports a limited transfer of elements between the dissolution and crystallisation sites. The two major conditions required to activate this mechanism are: (i) a stress deviator and (ii) the presence of a fluid phase that acts as solvent and as a medium for diffusion of solutes. The presence of a fluid phase is clearly demonstrated by the abundance of primary fluid inclusions in minerals sealing the quartz lenses like albite and apatite. Fluids probably originated from prograde metamorphic reactions that took place at the same time as deformation in the shear zones.

6.5. Formation of quartz lenses

Considering one phase of progressive deformation, three interpretations may be put forward to explain the parallelism of quartz lenses with S1 or S2 (Fig. 10):

1. Quartz crystallisation in voids created by S1 openings induced by S2 development during progressive rotation of cleavages parallel to shear plane (Fig. 10a). For such a mechanism, quartz lenses grow following a direction of 45° to S1 and to the contact between the quartz vein/surrounding rock.
2. Extensional fracture formed parallel to the shortening direction at a given time and then rotated towards the S2 plane by progressive shearing (Fig. 10b).
3. Hydraulic fracture formed initially parallel to S1 or S2 cleavage (Fig. 10c).

The geometrical observation of quartz veins demonstrates that some of them are parallel to S1 with plurimetric
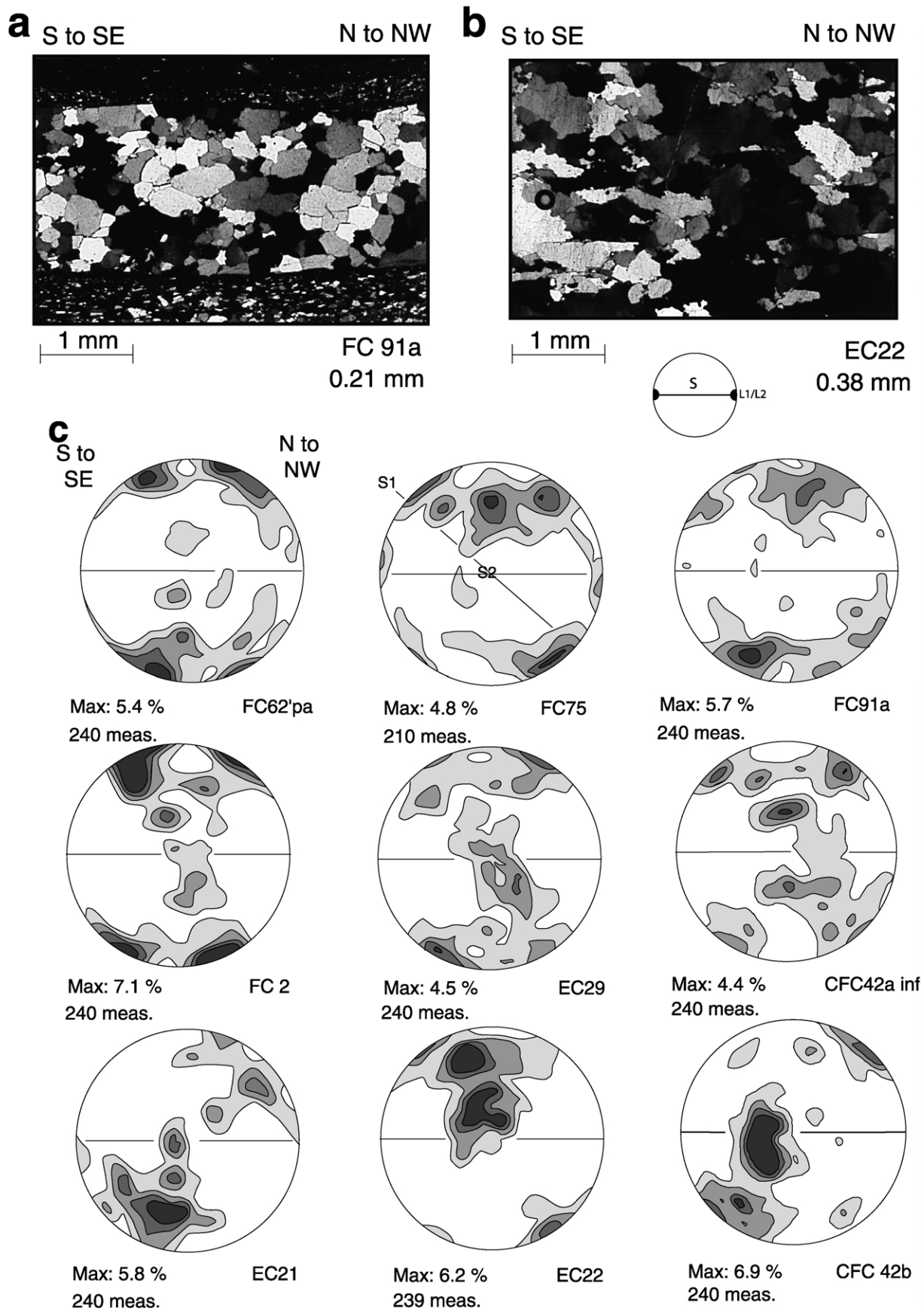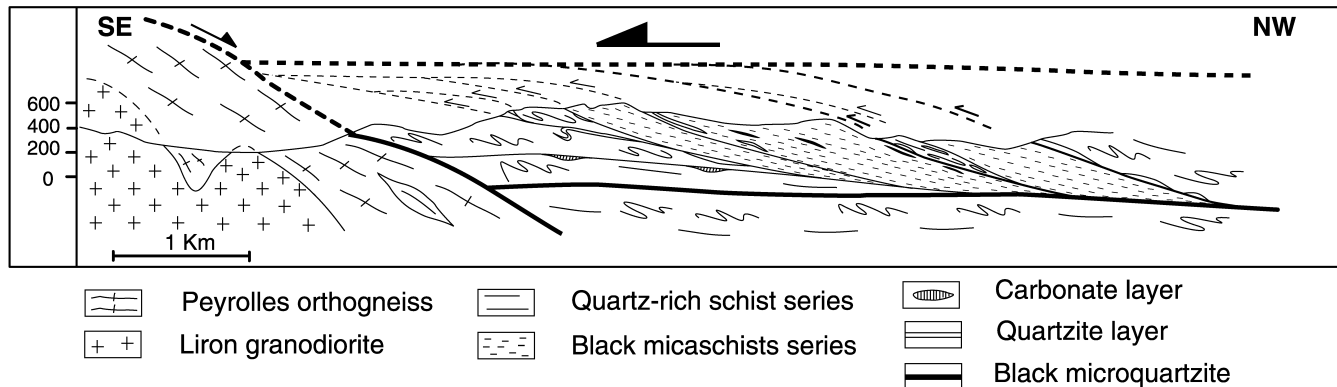
Fig. 9. Cross-section of the Cévennes area located on Fig. 1 (after Arnaud, 1997) interpreted after the schematic model of hinterland duplex formation from Boyer and Elliot (1982).

size in length and width and centimetric size in thickness. This geometry cannot be simply explained by the size of voids created by a process of décollement of the S1 induced by the development of S2 according to model 1 (Fig. 10a). In addition, no evidence for quartz growth at 45° to the wall-rock and cleavage have been observed.

The parallelism of the schist slivers with S1 and S2 of the wall-rock implies that they have been incorporated into the quartz lenses by opening of the cleavage planes. This observation excludes the lens rotation hypothesis (Fig. 10b). Geometry and internal microstructures in quartz lenses are more consistent with a lens formation by hydraulic fractures parallel to the cleavage (model 3, Fig. 10c).

We interpret the formation of quartz lenses by hydraulic fracturing and opening of the cleavage plane, which is a plane of high anisotropy and, therefore, of low strength, even if it is perpendicular to σ1 (Gratier, 1987; Fig. 10c). Formation of quartz veins by hydraulic fracturing parallel to a plane of anisotropy is a common interpretation in the literature (Fitches et al., 1986; Henderson et al., 1990; Cosgrove, 1993; Kennedy and Logan, 1997).

In such compressional tectonic context and for such pressure conditions of lens formation ($\pm$ 450 MPa), the fluid pressure corresponds to the lithostatic pressure. An hydraulic pressure will occur when $P_f > P_l + T_0$ (P_f being the fluid pressure, P_l, the lithostatic pressure and T_0 the tensile strength of the rock). The 'rosette' habit of minerals at the margins of some quartz lenses, the imbricate annular or 'caterpillar' shape of chlorite and the idiomorphism of numerous albite crystals suggest that these minerals were crystallising in open fractures and that the rate of lens aperture was faster than the rate of sealing by quartz (Cox, 1991). In this case, fluid pressure should have remained high enough in order to keep the cavity open, and minerals would have crystallised when the solution supersaturated in the

corresponding solutes. Quartz will crystallise with their $\langle c \rangle$ axis around the stretching direction (Hippertt, 1994), i.e. sub-parallel to the wall rock and cleavage. Orientation of quartz lenses, parallel to the sub-horizontal cleavage and bulk shear plane orientation does not favour fracture propagation and fluid circulation. This explained the composition of quartz lenses being directly controlled by that of the surrounding rock, which suggests either a limited fluid circulation or a short-distance transfer by diffusion within the intergranular fluid-film, between sites of dissolution and of crystallisation.

After their sealing, quartz lenses are deformed by intracrystalline processes, as indicated by the quartz $\langle c \rangle$ axis preferred orientation in fine-grained quartz lenses, and are dynamically recrystallised. However, dissolution–crystallisation seems to be the dominant deformation mechanism in these shear zones. The combination of dissolution–crystallisation and crystal plasticity processes is reported in quartz-rich rocks for transitional conditions of 15–20 km and 400–500 °C (Mitra, 1976; Hippertt, 1994).

7. Conclusions

- Recognition of schist shear zones allowed the definition of the main structural style of the Cévennes area and may be applied in other tectonic schist belts. Schist shear zones are up to 100 m thick. They contrast with the regional pattern through the presence of several cleavages, a stronger stretching lineation, non-cylindrical folds, boudinage structures, shear planes and numerous syn-tectonics quartz lenses.
- Mechanisms of deformation in these shear zones is dominantly dissolution–crystallisation. Dissolution is responsible for cleavage formation and crystallisation of dissolved elements in neighbouring quartz lenses.

Fig. 8. Microstructures (a,b) and typical c-axis PO of fine-grain quartz lenses (c). The $\langle c \rangle$ axis repartition and density contours (contours at 1, 2, 3, 4 and 8% per 1% area) have been reported on a Schmidt diagram (lower hemisphere) using the Fabric 7 program (Mainprice, 1992; unpublished). The EW line corresponds to the schistosity and the stretching lineation is horizontal in this plane. Samples FC91a and CFC 42b have type 'a' microstructures and others have type 'b' microstructures.
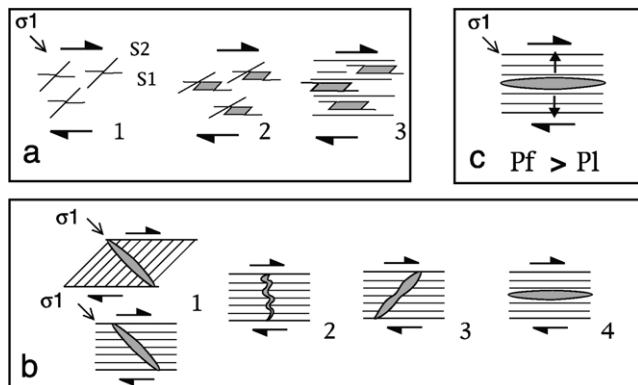
Fig. 10. Different hypotheses to explain the formation of quartz lenses parallel to the cleavage during a progressive deformation event. (a) Creation of voids during a shearing event (after Sauniac, 1980). (b) Extensional fracture and rotation towards the S2 cleavage. (c) Hydraulic fracturing parallel to the cleavage (after Gratier, 1987).

- Complementing other works in similar settings (Sauniac, 1981) and theoretical approaches (Bell and Cuff, 1989), dissolution–crystallisation acts over a large range of P–T conditions. In the Cévennes schists, these conditions have been determined as ca. ± 450 MPa and 500 °C.

- This study provides further evidence for the importance of fluids during deformation in monotonous schist series. Lithological variations in the series, like quartzite layers, induce shear zone localisation. During shearing deformation dissolution–crystallisation processes and metamorphic reactions produce overpressure in shear zones, which favours brittle behaviour of the rocks and may facilitate the thrusting process. This fluid overpressure enhances the formation of quartz lenses that occur at different stages of the shearing event. These quartz lenses form parallel to the foliation and are then deformed by crystal plasticity during the shearing event.

Acknowledgements

References

Alabouvette, B., Arthaud, F., Bodeur, Y., Barthes, J., Paloc, H., Aubague, M., 1988. Carte et notice explicative de la feuille le Vigan à 1/50,000. BRGM Map no. 937, scale 1:50,000.

Arnaud, F., 1997. Analyse structurale et thermo-barométrique d'un système de chevauchements varisque: les Cévennes centrales (Massif central français). Microstructures et mécanismes de déformation dans les zones de cisaillement schisteuses.Ph.D. thesis, INPL, University of Nancy.

Arnaud, F., Burg, J.P., 1993. Microstructures des mylonites schisteuses: cartographie des chevauchements varisques dans les Cévennes et détermination de leur cinématique. Comptes Rendus de l'Académie des Sciences (Paris) 11, 1441–1447.

Arthaud, F., 1970. Étude tectonique et microtectonique comparée de deux domaines hercyniens: les nappes de la Montagne Noire (France) et l'anticlinorium de l'Iglesiente (Sardaigne). Ph.D. thesis, University of Montpellier.

Arthaud, F., Mattauer, M., Matte, P., 1969. La direction des plis couchés penniques de la phase majeure hercynienne est sub-méridienne dans les Cévennes méridionales. Comptes Rendus de l'Académie des Sciences (Paris) 269, 556–559.

Bell, T., Cuff, C., 1989. Dissolution, solution transfer, diffusion versus fluid flow and volume loss during deformation/metamorphism. Journal of Metamorphic Geology 7, 425–447.

Berger, G.W., York, D., 1981. Geothermometry from ^{40}Ar/^{39}Ar dating experiments. Geochimica Cosmochimica Acta 45, 795–811.

Berthé, D., Brun, J.P., 1980. Evolution of folds during progressive shear in the south Armorican Shear Zone, France. Journal of Structural Geology 2, 127–133.

Berthé, D., Choukroune, P., Jégouzo, P., 1979. Orthogneiss, mylonite and non-coaxial deformation of granites: the example of the South Armorican Shear Zone. Journal of Structural Geology 1, 31–42.

Blumenfeld, P., Mainprice, D., Bouchez, J.L., 1986. ⟨C⟩ slip in quartz from subsolidus deformed granite. Tectonophysics 127, 97–115.

Boyer, S., Elliot, D., 1982. Thrust systems. American Association of Petroleum Geologists Bulletin 66, 1196–1230.

Brouder, P., 1968. De la présence de nappe plis de style pennique dans la série métamorphique hercynienne: les Cévennes, Massif central français. Comptes Rendus de l'Académie des Sciences (Paris) 267, 575–578.

Brouder, P., 1971. Les étapes de la formation d'un édifice hercynien polyphasé: les Cévennes. Comptes Rendus de l'Académie des Sciences (Paris) 273, 27–29.

Burg, J.P., Matte, P., 1978. A cross-section through the French Massif Central and the scope of its Variscan geodynamic evolution. Zeitschrift der Deutschen Geologischen Gesellschaft 129, 429–460.

Burg, J.P., Van Den Driessche, J., Brun, J.P., 1994. Syn- to post-thickening extension in the Variscan belt of Western Europe: modes and structural consequences. Géologie de la France 3, 33–51.

Caron, C., 1994. Les minéralisations Pb–Zn associées au Paléozoïque inférieur d'Europe Méridionale. Traçage isotopique Pb–Pb des gîtes de l'Iglésiente (SW Sardaigne) et des Cévennes et évolution du socle encaissant par la géochronologie U–Pb, ^{40}Ar/^{39}Ar et K–Ar. Ph.D. thesis, University of Montpellier.

Cosgrove, J.W., 1993. The interplay between fluids, folds and thrusts during the deformation of a sedimentary succession. Journal of Structural Geology 15, 491–500.

Costa, S., 1990. De la collision continentale à l'extension tardi-orogenique: 100 Ma d'histoire varisque dans le Massif central français. Une étude chronologique par la méthode ^{40}Ar–^{39}Ar. Ph.D. thesis, University of Montpellier.

Costa, S., Maluski, H., Lardeaux, J.M., 1993. ^{40}Ar–^{39}Ar chronology of Variscan tectonometamorphic events in an exhumed crustal nappe: the Monts du Lyonnais complex (Massif central, France). Chemical Geology 105, 339–359.

Coward, M.P., Potts, G.J., 1983. Complex strain patterns developed at the frontal and lateral tips to shear zones and thrust zones. Journal of Structural Geology 5, 383–399.

Cox, S.F., 1991. Geometry and internal structures of mesothermal vein system—implications for hydrodynamics and ore genesis during deformation. In: Structural Geology in Mining and Exploration. Extended Abstract 25. Geology Department (Key Centre) and University Extension, University of Western Australia, Nedlands, pp. 47–53.

Cox, S.F., Etheridge, M.A., 1983. Crack-seal fibre growth mechanisms and their significance in the development of oriented layer silicate microstructures. Tectonophysics 92, 147–170.

Cox, S.F., Etheridge, M.A., 1989. Coupled grain-scale dilatancy and mass transfer during deformation at high fluid pressures: examples from Mount Lyell, Tasmania. Journal of Structural Geology 11, 147–162.

Demay, A., 1931. Les nappes cévenoles. Mémoire explicatif de la Carte géologique Détaillée de la France. Imprimerie nationale.

Demay, A., 1948. Tectonique antéstéphanienne du Massif central. Mémoires de la Carte Géologique de France. Imprimerie nationale.

Dennis, A.J., Secor, D.T., 1987. A model for the development of crenulations in shear zones with applications from the Southern Appalachian Piedmont. Journal of Structural Geology 9, 809–817.

Djarar, H., Wang, H., Guiraud, M., Clermonté, J., Courel, L., Dumain, M., Laversanne, J., 1996. Le bassin stéphanien des Cévennes (Massif central): un exemple de relation entre sédimentation et tectonique extensive tardi-orogénique dans la chaîne varisque. Geodinamica Acta 9, 193–222.

Durney, D.W., 1972. Solution–transfer, an important geological deformation mechanism. Nature 235, 315–316.

Engel, W., Feist, R., Franke, W., 1981. Le Carbonifère anté-Stéphanien de la Montagne Noire: rapports entre mise en place des nappes et sédimentation. Bulletin du BRGM I, 341–389.

Etchecopar, A., 1977. A plane kinematic model of progressive deformation in a polycrystalline aggregate. Tectonophysics 39, 121–139.

Etchecopar, A., Vasseur, G., 1987. A 3-D kinematic model of fabric development in polycrystalline aggregates: comparison with experimental and natural examples. Journal of Structural Geology 9, 705–718.

Faure, M., 1995. Late orogenic carboniferous extensions in the Variscan French Massif Central. Tectonics 14, 132–153.

Fitches, W.R., Cave, R., Craig, J., Maltman, A.J., 1986. Early veins as evidence of detachment in the Lower Palaeozoic rocks of the Welsh Basin. Journal of Structural Geology 8, 607–620.

Gapais, D., Barbarin, B., 1986. Quartz fabric transition in a cooling syntectonic granite (Hermitage massif, France). Tectonophysics 125, 357–370.

Gardien, V., Lardeaux, J.M., Misseri, M., 1988. Les péridotites des Monts du Lyonnais (M.C.F.): témoins privilégiés d'une subduction de lithosphère paléozoïque. Comptes Rendus de l'Académie des Sciences (Paris) 307, 1967–1972.

Goffé, B., Murphy, W.M., Lagache, M., 1987. Experimental transport of Si, Al and Mg in hydrothermal solutions: an application to vein mineralization during high-pressure, low temperature metamorphism in the French Alps. Contributions to Mineralogy and Petrology 97, 438–450.

Gratier, J.P., 1984. La déformation des roches par dissolution–cristallisation. Aspects naturels et expérimentaux de ce fluage avec transfert de matière dans la croûte supérieure. Ph.D. thesis, University of Grenoble.

Gratier, J.P., 1987. Pressure solution–deposition creep and associated tectonic differentiation in sedimentary rocks. In: Jones, M.E., Preston, R.M.F. (Eds.), Deformation of Sediments and Sedimentary Rocks. Geological Society of London 29, pp. 25–38.

Guérangé-Lozes, J., 1987. Les nappes varisques de l'Albigeois cristallin (lithostratigraphie, volcanisme et déformations). Ph.D. thesis, University of Toulouse.

Guérangé-Lozes, J., Pellet, J., 1990. Carte et notice explicative de la feuille de Génolhac à 1/50 000. BRGM, Map no. 887, scale 1:50,000.

Henderson, J.R., Henderson, M.N., Wright, T.O., 1990. Water-sill hypothesis for the origin of certain veins in the Meguma Group, Nova Scotia, Canada. Geology 18, 654–657.

Hippertt, J.F.M., 1994. Microstructures and c-axes fabrics indicative of quartz dissolution in sheared quartzites and phyllonites. Tectonophysics 229, 141–163.

Kennedy, L.A., Logan, J.M., 1997. The role of veining and dissolution in the evolution of fine-grained mylonites: the McConnell thrust, Alberta. Journal of Structural Geology 19, 785–797.

Klaper, E., 1988. Quartz c-axis fabric development and large-scale post-nappe folding (Wandfluhhorn Fold, Penninic nappes). Journal of Structural Geology 18, 795–802.

Law, R.D., 1986. Relationships between strain and quartz crystallographic fabrics in the Roche Maurice quartzites of Plougastel, western Brittany. Journal of Structural Geology 8, 493–515.

Law, R.D., Schmid, S.M., Wheeler, J., 1990. Simple shear deformation and quartz crystallographic fabrics: a possible natural example from the Torridon area of NW Scotland. Journal of Structural Geology 12, 29–45.

Ledru, P., Lardeaux, J.M., Santallier, D., Autran, A., Quenardel, J.M., Floc'h, J.P., Lerouge, G., Maillet, N., Marchand, J., Ploquin, A., 1989. Où sont les nappes dans le Massif central français. Bulletin de la Société géologique de France 8, 605–618.

Lister, G.S., Dornsiepen, U.F., 1982. Fabric transitions in the Saxony Granulite Terrain. Journal of Structural Geology 4, 81–92.

Lister, G.S., Hobbs, B.E., 1980. The simulation of fabric development during plastic deformation and its application to quartzite: the influence of deformation history. Journal of Structural Geology 2, 355–370.

Lister, G.S., Snoke, A.W., 1984. S–C mylonites. Journal of Structural Geology 6, 617–638.

Magontier, J., 1988. Etude géologique de la Gardonenque, entre Saint-Jean-du-Gard et la Grand'Combe, à l'ouest d'Alès (Gard-France). Ph.D. thesis, University of Bordeaux.

Mainprice, D., Bouchez, J.L., Blumenfeld, P., Tubia, J.M., 1986. Dominant c slip in naturally deformed quartz: implications for dramatic plastic softening at high temperature. Geology 14, 819–822.

Marjoribanks, R.W., 1976. The relation between microfabric and strain in a progressively deformed quartzite sequence from Central Australia. Tectonophysics 32, 269–293.

Mattauer, M., Etchecopar, A., 1977. Argument en faveur de chevauchements de type Himalayen dans la chaîne hercynienne du Massif central français. Abstracts of Proceedings, CNRS, Paris 268, 261–267.

Matte, P., 1991. Accretionary history and crustal evolution of the Variscan belt in Western Europe. Tectonophysics 196, 309–337.

Mialhe, J., 1980. Le massif granitique de la Borne (Cévennes). Ph.D. thesis, University of Clermont-Ferrand.

Mitra, S., 1976. A quantative study of deformation mechanisms and finite strain in quartzites. Contributions to Mineralogy and Petrology 59, 203–226.

Munsch, H., 1981. Étude cartographique, pétrologique et structurale des séries métamorphiques d'un segment des Cévennes méridionales entre Saint-Jean-du-Gard et Saint-Germain-de-Calberte. Ph.D. thesis, University of Bordeaux.

Najoui, K., 1996. Conditions et âges de mise en place des granitoïdes de la zone externe sud du Massif central français: étude pétro-structurale et géochronologique ^{40}Ar–^{39}Ar des roches de leurs auréoles de contact. Implications géotectoniques. Ph.D. thesis, University of Montpellier.

Najoui, K., Leyreloup, A., Monié, P., 2000. Conditions et âges ^{40}Ar/^{39}Ar de mise en place des granitoïdes de la zone externe sud du Massif central français: exemple des granodiorites de St Guiral et du Liron (Cévennes, France). Bulletin de la Société Géologique de France 171, 495–510.

Passchier, C., Trouw, R., 1996. Microtectonics. Springer, Berlin.

Pellet, J., 1972. Données lithologiques et structurales sur les terrains cristallins cévenols affectés par l'accident de Villefort. Bulletin du Service de la Carte Géologique de France 282, 61.

Platt, J.P., Vissers, R.L.M., 1980. Extensional structures in anisotropic rocks. Journal of Structural Geology 2, 397–410.

Poirier, J.-P., Nicolas, A., 1975. Deformation induced recrystallization due to progressive misorientation of subgrains, with special reference to mantle peridotite. Journal of Geology 83, 707–720.

Quenardel, J.M., Santallier, D., Burg, J.P., Bril, H., Cathelineau, M., Marignac, C., 1991. Le Massif Central. Sciences Géologiques Bulletin 44, 105–206.

Ridley, J., 1986. Parallel stretching lineations and fold axes oblique to a shear displacement direction—a model and observations. Journal of Structural Geology 8, 647–653.

Sauniac, S., 1980. Mise en évidence de critères de cisaillement par les exsudats de quartz: exemple de la base de la nappe de Pardailhan (versant sud de la Montagne Noire). Revue de Géologie Dynamique et de Géographie Physique 22, 177–186.

Sauniac, S., 1981. Étude des exsudats syn-tectoniques liés à de grands

chevauchements, exemples de la Montagne Noire, de la Sardaigne S.E. et de l'Himalaya du N.W. Ph.D. thesis, University of Montpellier.

Schmid, S.M., Casey, M., 1986. Complete fabric analysis of some commonly observed quartz C-axis patterns. In: Hobbs, B.E., Heard, H.C. (Eds.), Mineral and Rock Deformation: Laboratory Studies. American Geophysical Union, Geophysical Monograph 36, pp. 263–286.

Schmid, S.M., Casey, M., Starkey, J., 1981. An illustration of the advantages of a complete texture analysis described by the orientation distribution function (ODF) using quartz pole figure data. Tectonophysics 78, 101–117.

Simpson, G., 1998. Dehydration-related deformation during regional metamorphism, NW Sardinia, Italy. Journal of Metamorphic Geology 16, 457–472.

Stallard, A., Shelley, D., 1995. Quartz c-axes parallel to stretching directions in very low-grade metamorphic rocks. Tectonophysics 249, 31–40.

Tullis, J.A., Christie, J.M., Griggs, D.T., 1973. Microstructures and preferred orientation of experimentally deformed quartzites. Geological Society of America Bulletin 84, 297–314.

Tullis, J.A., Stünitz, H., Teyssier, C., Heilbronner, R., 2000. Deformation microstructures in quartzo-feldspathic rocks. In: Means, W., Jessel, M., Urai, J. (Eds.), Stress, Strain and Structure. Journal of the Virtual Explorer 2.

Vialette, Y., Sabourdy, G., 1977a. Âge du granite de l'Aigoual dans le Massif des Cévennes (France). Comptes Rendu Sommaire de la Société Géologique de France XIX, 130–132.

Vialette, Y., Sabourdy, G., 1977b. Âge et origine des granitoïdes du Mont Lozère dans le Massif central français. Compte Rendu Sommaire de la Société Géologique de France XIX, 127–129.